PARTICLE PRODUCTION IN HEAVY-ION COLLISIONS*

GY. WOLF†

Institute for Nuclear Theory, University of Washington
Seattle, WA 98195, USA
and
GSI, D-64220 Darmstadt, Germany

(Received January 5, 1995)

We study γ, π- η- and vector-meson production in heavy-ion collisions. The dynamical evolution of the nucleus-nucleus collision is described by a transport equation of the Boltzmann-Uehling-Uhlenbeck type evolving phase-space distribution functions for nucleons, Δ's, $N(1440)$'s, $N(1535)$'s, π's and η's with their isospin degrees of freedom. Besides the dominant production of hard-photons in first chance n-p collisions a significant production of hard-photons in a later stage of heavy-ion collisions is predicted by BUU theory. The calculation predicts that the production of these photons strongly depend on the compressibility of the nuclear matter. Experimental indications for their production are found in the hard-photon energy spectra and the photon-photon correlation function measured at GANIL at energies 30-60.0 MeV/u. Furthermore, we present results for meson production in heavy-ion collisions at SIS energies. We show that the observed π's and η's are emitted dominantly at low density, on the other hand, vector-mesons provide a signal from the dense region of the reaction. They also contribute significantly to the dilepton invariant mass spectrum.

PACS numbers: 13.60.Le, 25.20.Lj, 25.40.Ve, 25.70.-z

---

* Presented at the XXIX Zakopane School of Physics, Zakopane, Poland, September 5–14, 1994.

† On leave from the CRIP, H-1525 Budapest, Hungary

1. Introduction

Heavy-ion collisions in the energy regime from a few tens of MeV/u up to about 2 GeV/u offer a possibility to study hot, dense nuclear matter far away from its ground state. At these energies both the individual nucleon-nucleon collisions and the nuclear equation of state (EOS) play important role.

Particle production may provide very valuable information about the violent phase of the reaction. It can be used to extract information about the EOS, to study the dynamics of heavy-ion collisions and to get information about medium effects like pion softening in nuclear matter, or decreasing vector-meson masses as the precursor of chiral restoration. In this paper we cover several aspects of particle production during a heavy-ion reaction.

We study heavy-ion collisions by use of a transport equation system of the Boltzmann–Uehling–Uhlenbeck type. We evolve phase-space distribution functions for nucleons, Δ's, $N(1440)$'s, $N(1535)$'s, π's and η's with their isospin degrees of freedom. For the production of other type of particles — photons and vector-mesons — we use the perturbative method [1]. In the collision term we put free cross-sections, the experimentally measured ones if available.

For interaction between particles we use a Skyrme-type mean-field potential, Coulomb force for charged particles, and Yukawa force to get right surface properties. This model (detailed description is given in [2–5] successfully describes the ground state of nuclei and, furthermore, correctly reproduces the experimental baryon spectra at 0.8 GeV/u [4], the pion and η numbers [5] and the transverse momentum spectra of π's [6] and η's [7]. Note that the low p_t part of the transverse momentum spectra of π's can be explained by the inclusion of the two-pion decay-channel of heavy resonances ($N(1440)$ and $N(1535)$) [6], which was failed before in several model calculations.

2. Equation of state and photon production

EOS by definition is the energy density e as a function of baryon density, ρ and entropy density, s. From $e(\rho, s)$ all the thermodynamical quantities can be calculated. In heavy-ion physics it is conventional to use $\varepsilon(\rho) = e/\rho$–m (= energy per baryon) instead of e.

Furthermore, for the sake of simplicity only the zero temperature, $T = 0$ ($s = 0$) section of $\varepsilon(\rho, s)$ is considered as equation of state. In the following we will use this restricted meaning of the EOS. Note, however, that in some

cases, e.g. in relativistic heavy-ion collisions the extrapolation to nonzero temperature (by assuming that the potential energy is independent of the temperature) may be questionable.

Beyond the vacuum point ($\rho = 0, \varepsilon = 0$) the saturation point is the most accessible and best known: the saturation density $= \rho_0 \approx 0.17$ fm^{-3}, the binding energy $= \varepsilon(\rho_0) = -16$ MeV and we know the first derivative of ε with respect to ρ at ρ_0 ($\partial\varepsilon/\partial\rho(\rho_0) = 0$, since it is the saturation point). Nowadays, lots of effort are spent to determine the second derivative of ε at ρ_0,

$$K = 9\rho_0^2 \left.\frac{\partial^2 \epsilon}{\partial \rho^2}\right|_{\rho_0}, \tag{1}$$

what is usually called as the incompressibility of nuclear matter.

There are two ways to determine the EOS. One may start with a realistic two-body nuclear force to describe nuclear matter, however, the way from the two-body problem to the nuclear matter one is not completely settled yet. Another possibility is to search for experimental information from nuclear many-body systems directly.

There are several approaches used to get information about the EOS [8]. Probably, the most certain value for K (which determines the EOS around ρ_0) were obtained by the analysis of the giant monopole resonance in nuclei. These studies concluded with: $K \approx 240$ MeV [9]. This value was later widely disputed in the literature, since according to some calculations *e.g.* [10] the fact, that supernovas exist, provides an evidence that the EOS must be soft ($K < 180$ MeV). However, higher order terms in density — having negligible effect around ρ_0 — may soften the EOS at very high densities, where the supernova explosion happens. Calculations of the transverse flow in heavy-ion collisions, on the other hand, seemed to indicate [11] a rather stiff EOS, but, as shown by [12–15], the not well-known momentum-dependence of the nucleon-nucleon interaction induces similar flow effects as a stiff EOS. So there is no final conclusion yet, and new independent methods to determine the incompressibility coefficient are very welcome.

2.1. Photon production

In heavy-ion collisions besides collective flow variables, the emission of particles, like nucleons, mesons, photons and dileptons may yield information about the EOS. Electromagnetic signals, photons and dileptons, are particularly promising probes of hot, dense matter, because they can leave the reaction volume essentially undistorted by final-state interactions. Since photons have much higher yield compared to dileptons they are experimentally favourable at low bombarding energies. However, the bombarding

energy domain in which hard-photons can be used as probes is restricted to intermediate energies below roughly 100 MeV/u where the contribution of photons from neutral pion decay is still weak. We propose the energy spectra of photons to be sensitive on the EOS [16].

From the extended experimental data and from dynamic phase-space simulations [2, 3, 17] the dominant source of hard-photons, *i.e.*, photons with energies larger than 30 MeV, has been attributed to the bremsstrahlung emitted in first-chance proton-neutron collisions. At intermediate energies where the bombarding energy is comparable to the Fermi energy, hard-photons probe the phase-space distribution of the nucleons in the collision zone and convey information on the dynamics of the collision in its early stage [18].

Aside of the aforementioned dominant source which produces what we shall call *direct* hard-photons, BUU calculations [2] have predicted the existence of a second source of n-p bremsstrahlung photons occurring at a later stage of the heavy-ion collision when the system is almost fully thermalyzed. The photons originating from this source may be called *thermal* hard-photons [16].

At low intermediate energies, typically below 50 MeV/u for a symmetric system, the dominant reaction mechanism in central heavy-ion collision is the incomplete fusion. In the first stage of the collision a dense system is formed ($\rho \sim 1.4\rho_0$) which then slowly expands until the point the attractive part of the nuclear force is strong enough to drive a second compression of the system. The system subsequently undergoes then oscillations around the saturation density and a hot nucleus is formed. The strength of the restoring force (attractive below ρ_0 and repulsive above) depends on the incompressibility of nuclear matter K: for large K the restoring force is larger than for small K (Fig. 1), so the second compression produces higher densities for larger K. At higher bombarding energies the expansion is sufficiently violent to break the system in many fragments and no thermal hard-photons are produced.

The computed production rate of hard-photons of energy 30, 80 and 130 MeV are shown as the function of the collision time in Fig. 2. It was calculated for the system ^{181}Ta $+^{197}$Au at 40, 60 and 90 MeV/u laboratory energies and for the mean average impact parameter $b = 5$ fm. The cross-section for the $n + p \rightarrow n + p + \gamma$ reaction was taken from Ref. [19]. The existence of two hard-photon sources is clearly marked because of the absence of photon production during the time the system undergoes the expansion. As expected the thermal hard-photon production decreases with increasing beam energy and almost disappears at the 90 MeV/u indicating that the system has fragmented. The figure indicates also a radical difference in the energy spectra of the photons from the two sources, the thermal

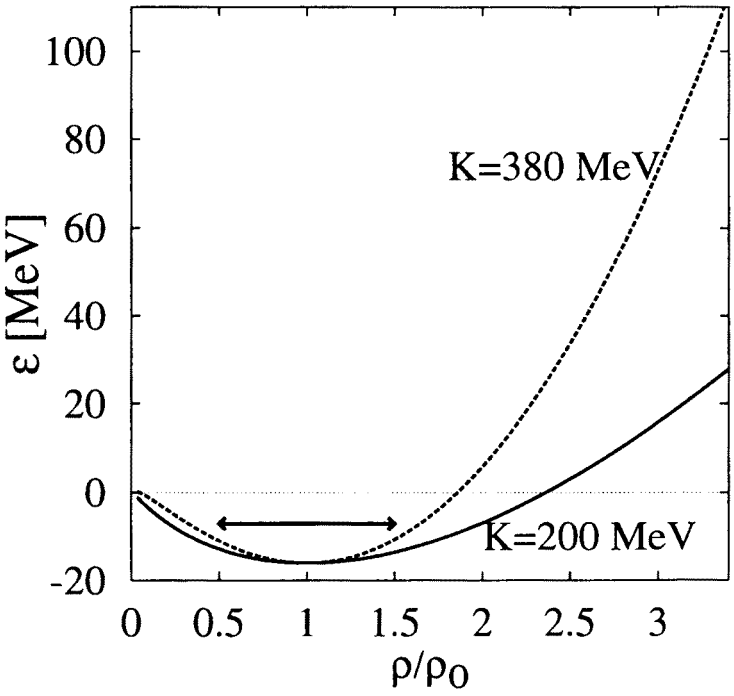

Fig. 1. Soft (solid line) and hard (dashed line) equation of state for nuclear matter in a Skyrme parameterization. The arrow indicates the oscillation of a compound system at a bombarding energy of 30 MeV/u.

hard-photons having a softer spectra than the direct ones. This reflects the fact that in the later stage of the collision the energy available in the center of mass of neutron-proton collisions is, on average, smaller than at the beginning of the collision. By describing the spectra by an exponential shape with an inverse slope parameter E_0, the BUU simulations predict that $E_0^{\text{direct}}/E_0^{\text{thermal}} \approx 2 - 2.5$.

Most importantly the calculations predict that the production rate of the thermal hard-photons is very sensitive to the incompressibility modulus K of infinite nuclear matter since the density oscillations themselves are sensitive to K. This is demonstrated in Fig. 3 where the production rate of hard-photons is shown as a function of the collision time calculated for two values of K (200 and 380 MeV) in the system ^{181}Ta $+^{197}$Au at 40 MeV/u and $b = 5$ fm. Since direct hard-photons are produced in *first chance* neutron-proton collisions their production rate does not depend on K.

The thermal photon production rate varies strongly with K by up to a factor 3 between the two extreme values of K that we have selected. Such a strong variation implies that the measurement of thermal hard-

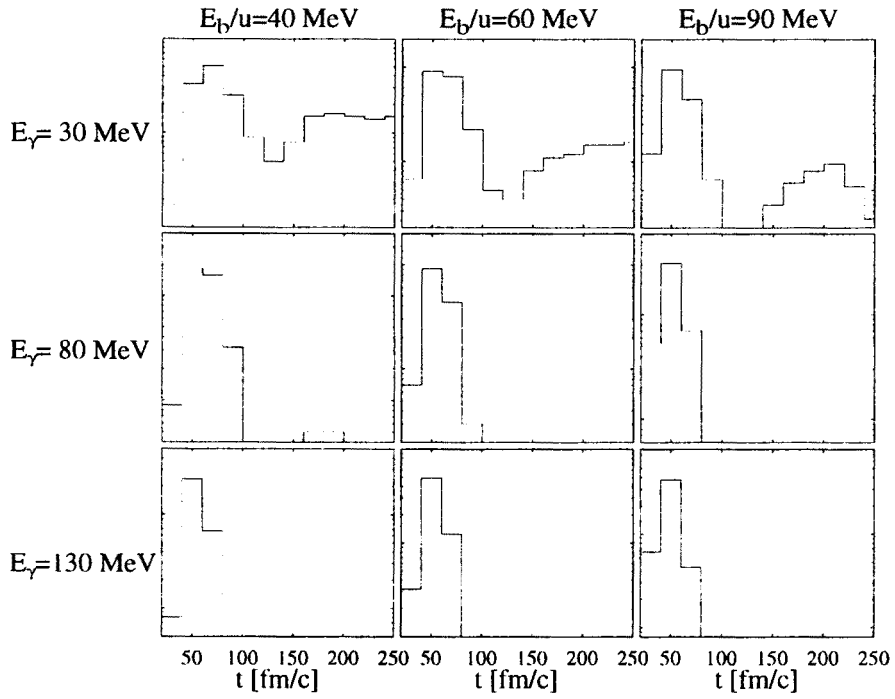

Fig. 2. Production rate of photons with energies of 30, 80 and 130 MeV obtained with BUU for the system ^{181}Ta $+^{197}$Au at 40, 60 and 90A MeV. The impact parameter was $b = 5$ fm.

photons provides a new and sensitive method to determine the incompressibility modulus of nuclear matter. It should be emphasized that K is deduced from the relative yield of thermal to direct hard-photons thus making this method almost independent of the choice of the nucleon-nucleon cross-section. Moreover, here the uncertainty corresponding to the unknown momentum-dependent force and the parameterization of the mean-field potential (which is also uncertain above ρ_0) do not play any role.

Experimentally there are two indications for the existence of these thermal hard-photons: one the hand, the energy spectra of inclusive hard-photons [16] show a two-slope behaviour and on the other, the photon-photon correlation function shows an oscillation as a function of $Q_{\mathrm{inv}} = \sqrt{(p_1 - p_2)^2}$ [20]. Both phenomena can be explained by two photon sources. The photons were detected and identified with the photon spectrometer TAPS [18, 21].

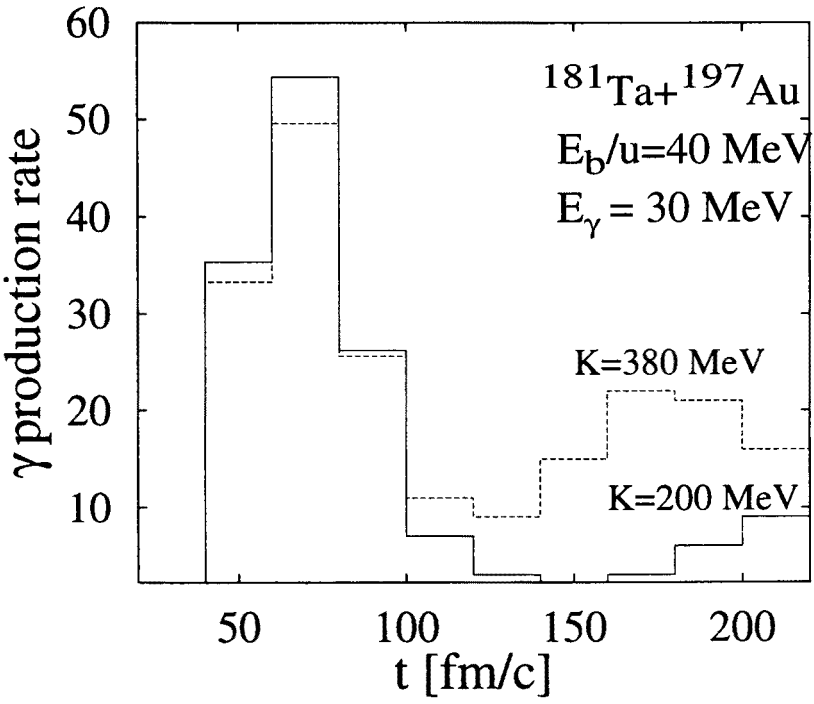

Fig. 3. Production rate of photons with an energy of 30 MeV as a function of the incompressibility K_∞ of nuclear matter obtained with BUU for the system ^{181}Ta $+^{197}$Au at 40A MeV and $b = 5$ fm.

3. Meson production

3.1. π and η dynamics

We show in Fig. 4 the baryonic decomposition for the highest density region (maximal resonance/nucleon ratio) in the central cell ($\approx 33\text{fm}^3$) of the reaction volume for central ^{197}Au $+^{197}$Au reaction as a function of the bombarding energy per nucleon. It is clearly seen that about 30% of all baryons are Δ's around 2 GeV/u, whereas the population of the higher-lying resonances is small. Since the maximum density in this cell is about 3 times that of ground state nuclear matter (ρ_0), this result indicates a Δ density of about $0.8 - 1\rho_0$. According to the calculation in this stage of the collision the pion density is equal to the density of the $N(1440)$-resonance.

In Fig. 5 we show the time evolution of the $\Delta, N(1535), \eta$ and π yields in comparison to the density of the central region (thick solid line). The number of "excitations" (the sum of mesons and resonances) reaches its

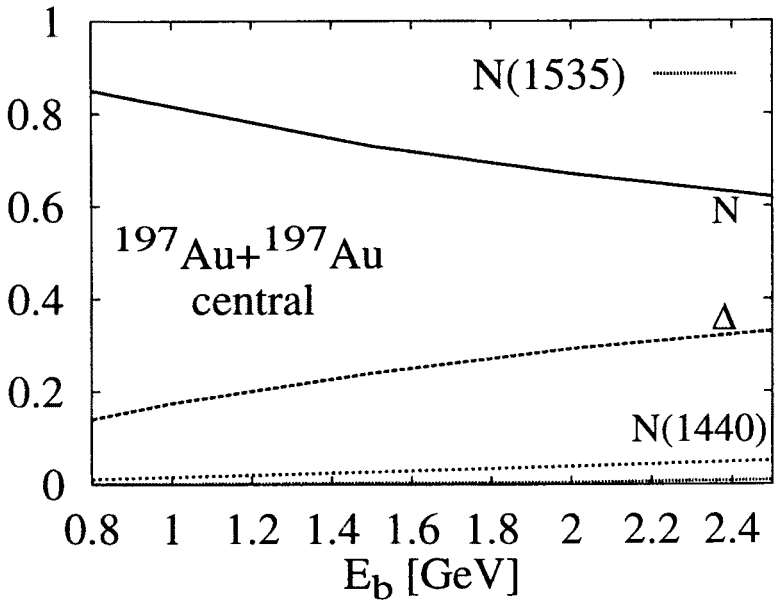

Fig. 4. Baryon decomposition at the highest densities in a central cell of volume 33fm^3 for head-on collisions of Au+Au as a function of the bombarding energy per nucleon.

final value already in the dense phase, where almost all "excitations" are resonances. The meson yields, on the other hand, reach their final values only in the expansion stage, where the η's decouple from the baryons earlier than the pions. Furthermore, η's are produced at higher energy density than pions due to the substantially larger threshold involved.

In Fig. 6 we show the distribution of the collision numbers for the asymptotically observed π's and η's in a central collision of ^{197}Au $+^{197}$Au at 1 GeV/u. In this context a "collision" for a meson means an absorption and a subsequent reemission for the same type of meson. For π's the distribution is rather flat and there are pions with relatively high collision numbers of 10–12 while the average collision number for pions is $\approx$ 5–6. For η's the distribution of collision numbers falls down much faster, because $N(1535)$'s decay only with $\approx$ 50% probability to η's whereas the Δ's and $N(1440)$'s decay with almost 100% probability to pions.

For ^{40}Ca $+^{40}$Ca and ^{197}Au $+^{197}$Au at 1 and 2 GeV/u bombarding energies we compare in Fig. 7 the density dependence of η and π creation to the density dependence of those η's (η_f) and π's (π_f) which actually leave the system. For each reaction the majority of η's are produced (dot-dashed line) at high density; however, for η's reaching the detector the density

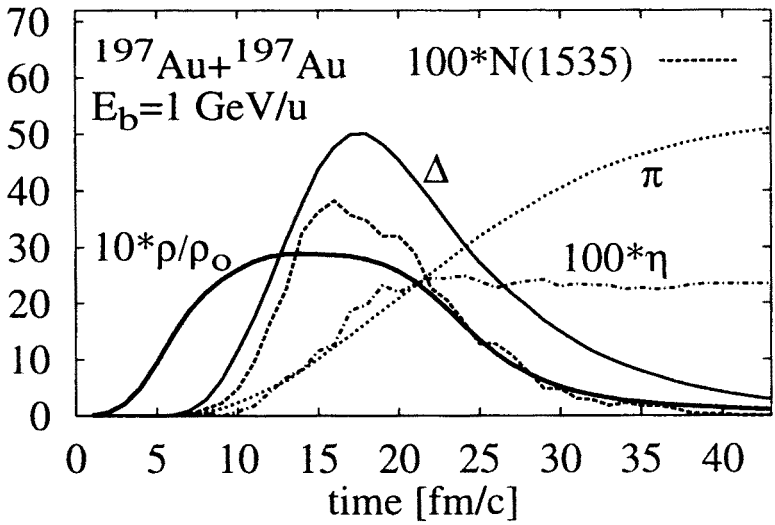

Fig. 5. Time evolution of various quantities in a central collision of ^{197}Au $+^{197}$Au at 1 GeV/u: The central density ρ (thick solid line); the number of Δ's (solid line), $N(1535)$'s (dashed line), η's (dash-dotted line), and π's (dotted line). The number of η's and $N(1535)$'s are scaled by a factor of 100 and the central density is scaled by a factor of 10.

dependence of the production is rather flat. The situation is similar for pions, but there is an extra peak at small densities which is much more pronounced at the higher energy of 2 GeV/u. The explanation is obvious: due to the strong resonance absorption for both the mean-free path of the mesons is small such that the high density peak is suppressed. That the final η's have a broader density distribution reflects the fact that they experience less rescattering than the pions.

All these results show that inclusive π and η measurements cannot be used to study the hot, dense zone of the collision. Because of the strong rescattering they can carry information only about the low density region of the system.

3.2. Vector-meson production

In order to get information about the high density phase of a reaction such a signal should be chosen which is very subthreshold at the given energy (so if *e.g.* π's then the energetic ones). Above threshold the production from low density phase usually overwhelms that of from high density. Vector-mesons, having their threshold in pp collision at $E_b \approx 1.9$ GeV, are good

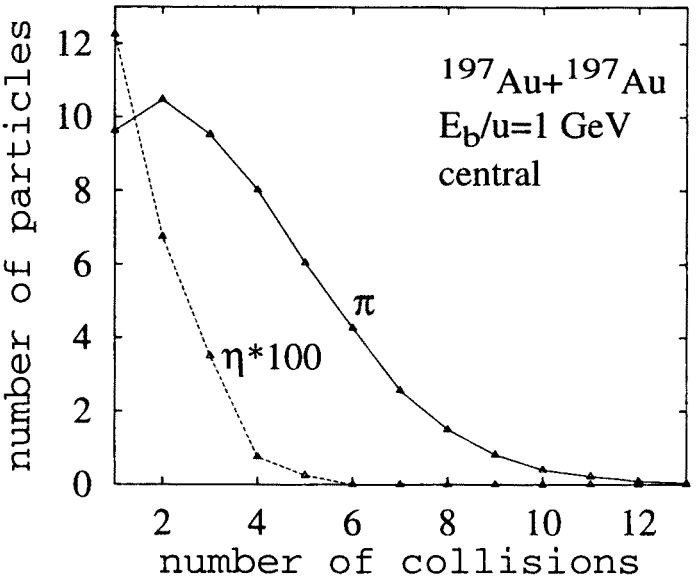

Fig. 6. The collision number distribution for asymptotic η's (dashed line), and π's (solid line) in a central collision of ^{197}Au $+^{197}$Au at 1 GeV/u. The number of η's is scaled by a factor of 100.

candidates for probing the high density phase of heavy-ion collisions at SIS energies.

The experimental $pp \to pp\omega$ and $pp \to pp\rho$ cross-sections are fitted (Fig. 8) by

$$\sigma^{pp\to pp\omega} = 0.36\frac{(\sqrt{s}-\sqrt{s_0})\text{GeV}}{1.25\text{GeV}^2+(\sqrt{s}-\sqrt{s_0})^2}[\text{mb}]$$
$$\sigma^{pp\to pp\rho} = 0.24\frac{(\sqrt{s}-\sqrt{s_0})\text{GeV}}{1.4\text{GeV}^2+(\sqrt{s}-\sqrt{s_0})^2}[\text{mb}] \qquad (2)$$

and used in our calculation. We put the same elementary cross-sections for each isospin channel, furthermore,

$$\sigma^{\Delta\Delta} = 0.5\sigma^{NN} \qquad \text{and} \qquad \sigma^{\Delta N} = 0.75\sigma^{NN}.$$

In Fig. 9 the p_t spectrum of the ω-meson is shown in ^{197}Au $+^{197}$Au at 1 GeV/u bombarding energy. The dominant contributions come from the $N\Delta \to NN\omega$ and from the $NN^* \to NN\omega$ channels since below threshold energies very few NN collisions have enough energy for the production of an ω. On the other hand, in the case of NR (R : Δ or N^*) collisions the mass difference of the resonance and the nucleon lowers the necessary kinetic energy for ω production. Similar effect has been observed in η [5], kaon [22–24]

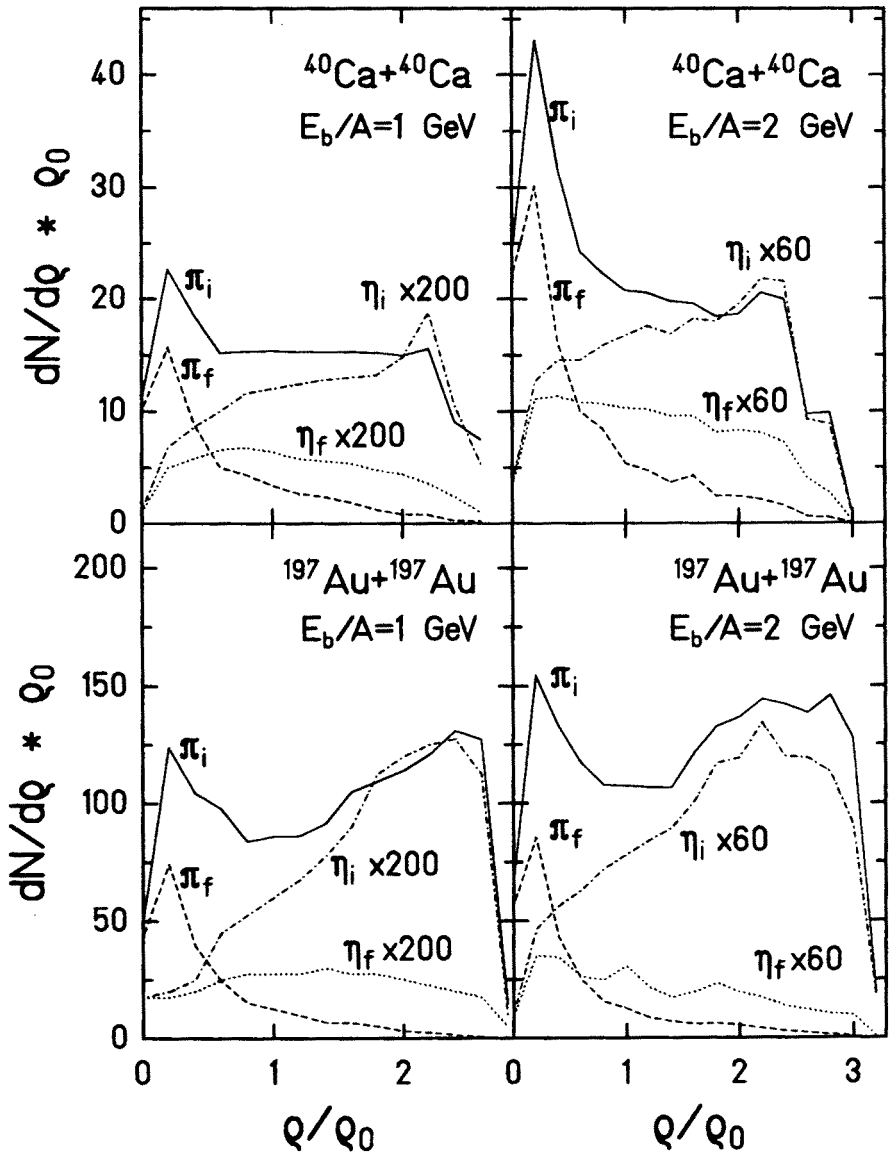

Fig. 7. Initial π (solid lines) and η (dash-dotted lines) numbers (π_i, η_i) as a function of the density at their creation point for $^{40}Ca + ^{40}Ca$ and for $^{197}Au + ^{197}Au$ at 1 and 2 GeV/u in comparison to the density dependence of the final mesons (π_f, η_f) that have escaped from the reaction volume.

and antiproton [25–28] production. The general trend can be summarized as: above threshold energies most mesons are produced in NN collisions,

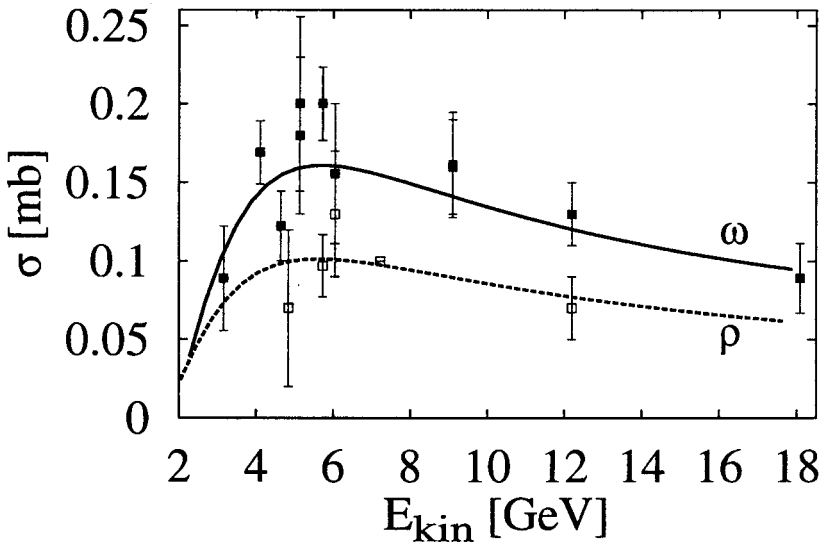

Fig. 8. Fit for $\sigma^{pp\to pp\omega}$ (experimental data: full squares; fit: solid line) and for $\sigma^{pp\to pp\rho}$ (experimental data: empty squares; fit: dotted line).

however, much below threshold NR collisions are dominating the production. (It is interesting to note that in proton-nucleus collisions, however, the πN channel is dominating the production of subthreshold particles.)

We show the result of the calculation for the density dependence of vector-meson production in ^{197}Au $+^{197}$Au at 1 GeV/u bombarding energy in Fig. 10. We find as we expected that at such subthreshold energies ω and ρ productions are peaked at rather high densities ($\approx 2.4\rho_0$).

Vector-mesons have rather large decay width to e^+e^- pairs. It was shown [4, 29] that at SIS energies the dominant contribution to the dileptons with high invariant masses ($M > 500$ MeV) are coming from ρ-decay via the $\pi^+\pi^- \to \rho \to e^+e^-$ channel. The contribution of the omega meson peaks out of the annihilation background (Fig. 11). This gives a good opportunity to observe the ω-meson. However, the experimental set up should have very good mass resolution to observe this narrow peak. If one averages this contribution over 50 MeV mass bin (what was the mass resolution of the DLS spectrometer at BEVALAC), the peak completely disappears. The drawback of probing the dense medium by the ω-meson is that its lifetime in vacuum is much larger than the whole reaction time. If it does not broaden substantially in medium then it decays outside of the reaction volume loosing the information about its medium properties. In our calculation the contribution of the $b+b \to \rho \to e^+e^-$ channel (b denotes a baryon) is negligible.

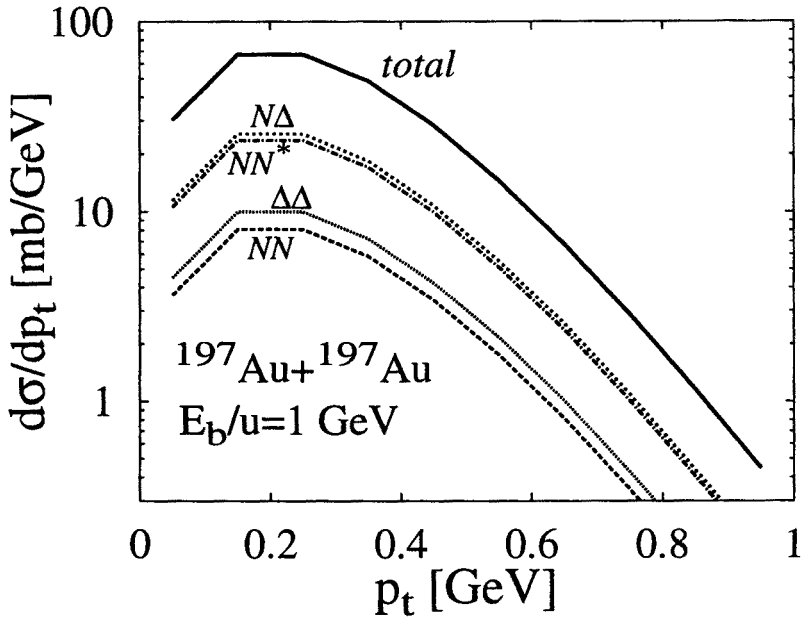

Fig. 9. p_t spectrum for the ω meson in ^{197}Au $+^{197}$Au collision at 1 GeV/u bombarding energy. The various contributions are indicated in the figure.

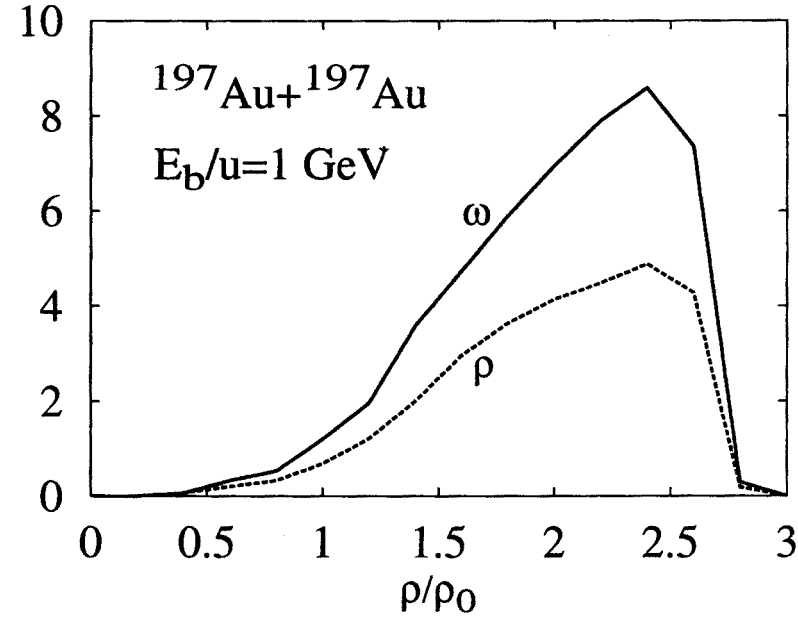

Fig. 10. Vector-meson production as a function of density in a central ^{197}Au $+^{197}$Au collision at 1 GeV/u bombarding energy.

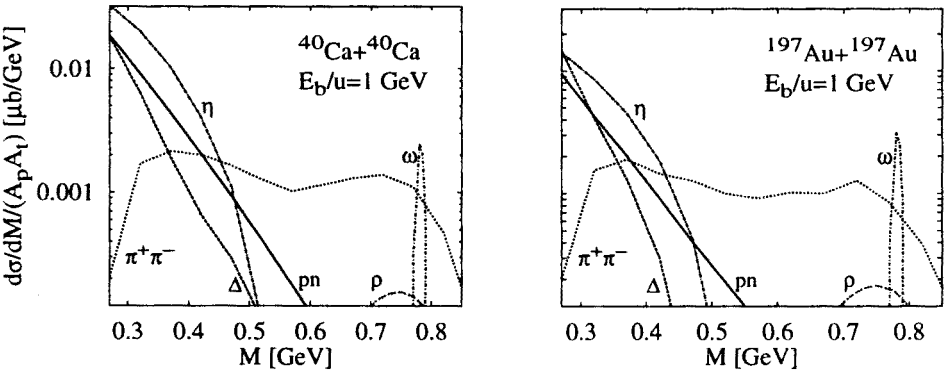

Fig. 11. Dilepton invariant mass spectra for ^{40}Ca $+^{40}$Ca and for ^{197}Au $+^{197}$Au at 1 GeV/u bombarding energy. Solid line: *pn* bremsstrahlung; dot-dashed: η Dalitz-decay, dotted: $\pi^+\pi^-$ annihilation; dashed: Δ Dalitz-decay; dot-dashed: ω-decay; and dotted: ρ-decay.

4. Summary

We have studied heavy-ion reaction dynamics on the basis of a microscopical model of the BUU type. In this model the nucleons, baryonic resonances, the $\Delta(1232)$, the $N(1440)$ and the $N(1535)$ as well as pions and η's are explicitly propagated.

We have shown that BUU calculations predict in the energy range of 30-60 MeV/u besides the dominating first chance np bremsstrahlung a significant production of thermal hard-photons which are emitted in a later stage of the collision from a nearly thermal-source. We have suggested a promising method, independent of the choice of the nucleon-nucleon cross section, to measure the incompressibility modulus of infinite nuclear matter using the production rate of thermal hard-photons.

At subthreshold energies the dominant source of produced particles, like η's, kaons, antiprotons and vector-mesons, are nucleon+resonance (Δ or N^*) collisions. Although the resonance to nucleon ratio is still smaller than 0.5, the mass difference of the resonance and the nucleon lowers the necessary kinetic energy for the production of the particles, increasing the production probability in this channel.

We have shown that most of the η's and pions leaving the system are produced at rather low densities so that they are not well suited to study the high density phase of the reaction. On the other hand, heavy mesons like vector-mesons are produced dominantly in the dense region, since the energy/particle is only there high enough to have significant probability of

energetic collisions. Vector-mesons, dominating the dilepton invariant mass spectra at the high mass region, giving a good opportunity to observe their behaviour at high density.

The subsection on γ production is based on the work done in collaboration with G. Martínez, F.M. Marqués and Y. Schutz. The subsection on π and η dynamics is the result of the collaboration with W. Cassing, U. Mosel and S. Teis. I wish to thank their contributions.

REFERENCES

[1] G.F. Bertsch, S. Das Gupta *Phys. Rep.* **160**, 189 (1988).
[2] K. Niita, W. Cassing, U. Mosel, *Nucl. Phys.* **A504**, 391 (1989).
[3] W. Cassing, V. Metag, U. Mosel, K. Niita, *Phys. Rep.* **188**, 363 (1990).
[4] Gy. Wolf *et al.*, *Nucl. Phys.* **A517**, 615 (1990).
[5] Gy. Wolf, W. Cassing, U. Mosel, *Nucl. Phys.* **A552**, 549 (1993).
[6] S. Teis, Gy. Wolf *et al.*, in preparation.
[7] S. Teis, Gy. Wolf *et al.*, in preparation.
[8] N.K. Glendenning, *Phys. Rev.* **C37**, 2733 (1988).
[9] J.P. Blaizot, *Phys. Rep.* **64**, 171 (1980).
[10] E. Baron, J. Cooperstein, S. Kahana, *Phys. Rev. Lett.* **55**, 126 (1985).
[11] J.J. Molitoris, D. Hahn, H. Stöcker, *Nucl. Phys.* **A447**, 13c (1985).
[12] C. Gale, G.F. Bertsch, S. Das Gupta, *Phys. Rev.* **C35**, 1666 (1987).
[13] J. Aichelin *et al.*, *Phys. Rev. Lett.* **58**, 1926 (1987).
[14] C.M. Ko, Q. Li, *Phys. Rev.* **C37**, 2270 (1988).
[15] W. Cassing, A. Lang, S. Teis, K. Weber, *Nucl. Phys.* **A545**, 123c (1992).
[16] G. Martínez *et al.*, submitted to *Phys. Lett.* **B**.
[17] H. Nifenecker, J.A. Pinston, *Prog. Part. Nucl. Phys.* **23**, 271 (1989).
[18] G. Martínez *et al.*, *Phys. Lett.*, **B334**, 23 (1994).
[19] M. Schäfer *et al.*, *Z. Phys.* **A339**, 391 (1991).
[20] F.M. Marqués *et al.*, submitted to *Phys. Lett.* **B**.
[21] F.M. Marqués *et al.*, *Phys. Rev. Lett.* **73**, 34 (1994).
[22] A. Lang *et al.*, *Nucl. Phys.* **A541**, 507 (1992).
[23] S.W. Huang *et al.*, *Phys. Lett.* **B298**, 41 (1993).
[24] X.S. Fang *et al.*, *Nucl. Phys.* **A575**, 766 (1994).
[25] G. Batko *et al.*, *Phys. Lett.* **B256**, 331 (1991).
[26] G.Q. Li, C.M. Ko, X.S. Fang, Y.M. Zheng, *Phys. Rev.* **C49**, 1139 (1994).
[27] C. Spieles *et al.*, *Mod. Phys. Lett.* **A27**, 2547 (1993).
[28] S. Teis *et al.*, *Phys. Rev.* **C50**, 388 (1994).
[29] L. Xiong, Z.G. Wu, C.M. Ko, J.Q. Wu, *Nucl. Phys.* **A512**, 772 (1990).